

Anomalous magnetic response of the valence-fluctuating compound YbInCu_4

J. K. Freericks and V. Zlatić[†]

Department of Physics, Georgetown University, Washington, DC 20057

(November 27, 2018)

The exact solution of the spin one-half Falicov-Kimball model, with random hopping between the lattice sites, is used to explain the anomalous magnetic response of Yb-based valence-fluctuating intermetallic compounds. The anomalous behavior arises from an entropy-driven local-moment–nonmagnetic transition of unhybridized Yb ions in these materials which can also be used to explain the observed metamagnetism and resistivity anomalies.

The valence-fluctuating (VF) compounds YbInCu_4 , $\text{YbIn}_{1-x}\text{Ag}_x\text{Cu}_4$ and $\text{Yb}_{1-x}\text{In}_x\text{Cu}_2$ exhibit large anomalies in their thermodynamic [1–3], spectroscopic [1,4,5] and transport properties [1,3,6], around a characteristic, sample-dependent temperature T_V (30 – 70K). The anomalies are due to the VF, as the L_{III} -edge, Mössbauer, X-ray absorption and the thermal-expansion data show that the Yb ions fluctuate between a 2+ and 3+ state. However, the atomic volume is altered at T_V by a small amount and the average valence of the Yb ions [1,3,5] does not change by more than 4%. The X-ray and neutron data do not show any structural changes across the VF transition [3,4,6,7], and the neutron [4] and the NMR data [2] rule out magnetic ordering as a possible explanation of the anomalous behavior. Here, we focus on the anomalous magnetic response of Yb-based VF compounds, as revealed by the temperature dependence of the low-field susceptibility, $\chi(T)$, and the field-induced torque, $\Gamma(T)$, and by the measurements of the high-field magnetization, $M(H)$, at temperatures below T_V .

The anomaly in $\chi(T)$ is seen most clearly in the YbInCu_4 single-crystal data [3], as a pronounced asymmetric peak just above T_V . The anomalous peak rises from a large uniform background and is much steeper on the low-temperature than on the high-temperature side. Below T_V , $\chi(T)$ drops to a minimum and then grows slowly towards the lowest temperatures, where a weaker Curie-like upturn is often seen. For $T \gg T_V$, $\chi(T)$ decays in a Curie-Weiss fashion but the magnitude of the susceptibility at 300 K is about the same as at the low-temperature minimum. Surprisingly, the magnitude, and even the sign, of the Curie-Weiss temperature appears to

be sample dependent. Such behavior is quite different from what one finds in a typical metallic heavy-fermion sample, like YbAgCu_4 [10,2], where the low-temperature response is much enhanced over the room-temperature one and $\chi(T)$ exhibits a shallow and symmetric maximum.

The torque induced by the field (measured for the single crystals used in Ref. [3]) shows that the magnetic susceptibility is also anisotropic [9], which is quite unusual for compounds of cubic symmetry. The torque, $\Gamma(T)$, is characterized by an asymmetric peak, which is clearly related to the anomalous peak in $\chi(T)$. Below T_V , $\Gamma(T)$ drops by several orders of magnitude and then, like $\chi(T)$, it shows an upturn as the temperature is further reduced. The decay of $\Gamma(T)$ above T_V is very rapid and cannot be described by a Curie-Weiss law. The Γ -anomaly, like the χ -anomaly, is sharper and more asymmetric for the samples with lower T_V 's.

The anomaly in the high-field magnetization of YbInCu_4 and $\text{YbIn}_{1-x}\text{Ag}_x\text{Cu}_4$ [2,8] is characterized by a sudden increase of the slope and the saturation of $M(H)$ at about $H_V \simeq 30 - 50 T$. The magnetostriction data [2] indicate that the metamagnetism relates to valence fluctuations of Yb ions but the field-induced change in the average f-count, $\langle n_f \rangle$ is even smaller than the temperature-induced one. At low temperatures, the Zeeman energy at H_V is comparable to the thermal energy at T_V . At elevated temperatures, the metamagnetic transition is absent [4]. The magnetic anomalies at T_V and H_V , and the characteristic energies $k_B T_V$ and $\mu_B H_V$ are sample dependent [2], while the low-field response, for $T < T_V$, is quite robust with respect to doping and annealing.

The simultaneous analysis of the susceptibility and the torque data shows [9] that the magnetic response is due to two physically distinct components. The first one, χ_{VF} , is large (on an absolute scale), isotropic, and sample independent. The second one, χ_{local} , is vanishingly small below T_V and smaller than χ_{VF} at high temperatures, but dominates $\chi(T)$ and $\Gamma(T)$ near T_V . χ_{local} is anisotropic and strongly sample dependent. In addition, the field and sample dependence of the $M(H)$ data also supports the picture of two types of magnetic excitations.

To explain these features we recall that the Yb compounds mentioned above crystallize in $C15b$ -(AuBe_5)-type structure [4,7] with In and Yb ions at the so-called 4a and 4c sites, respectively. Because of the short 4a-4c distance, the f-states of the Yb ions hybridize with the In ions and give rise to an enhanced background susceptibility, χ_{VF} , which dominates $\chi(T)$ much above and

© 1996 by the authors. Reproduction of this article by any means is permitted for non-commercial purposes.

below T_V . For $T \leq T_V$, these hybridized states also yield the sample-independent low-field magnetization. On the other hand, the disordered C15-type structure, in which the 4a and 4c sites are randomly occupied by Yb and In ions, is quite close to the C15b-type structure, and is not ruled out by the X-ray and neutron data [4,7] (especially for a small number of disordered Yb ions occupying the In 4a sites). Thus, we assume that a small number (N) of Yb ions in YbInCu₄ occupy the In 4a sites *and that their 4f-states remain unhybridized*. The hybridization between these ill-placed 4a-Yb ions and the regular 4a-In ions is absent because the 4a-4a distance is nearly twice the 4a-4b distance. The magnetization, of the 4a-Yb ions in the f^{13} configuration is angle-dependent, because the g -factor of the unhybridized f -holes becomes anisotropic in the distorted crystal environment. The external field induces the torque, which relates to the local susceptibility as, $\Gamma \simeq \frac{\Delta g^2}{\langle g^2 \rangle} \langle \chi_{local}(N, T) \rangle H^2$, where $\Delta g^2 = g_x^2 - g_y^2$ is the g -factor anisotropy between the x and y direction, and $\langle \dots \rangle$ denotes the angular average. As show below, the unhybridized Yb ions crossover at T_V from the magnetic 3+ to the nonmagnetic 2+ configuration, so that χ_{local} and Γ vanish. At low temperatures and high fields the unhybridized states lead to the metamagnetic transition with a small energy difference between the low-field and the high field states. Note, $\langle n_f \rangle$ does not change much either at H_V or at T_V , because the VF transition involves only N 4a-impurities out of a total of N_l Yb ions, i.e. $N/N_l \ll 1$.

Our model for the anomalous magnetic response of these materials begins with this assumption that the f -electrons of the disordered Yb ions are *not* hybridized with the rest of the lattice. These ions form a random lattice. The conduction electrons can move, via nearest-neighbor hopping on the regular lattice, between any of these random lattice sites; i.e. the system can be modeled by localized f -states at energy E and delocalized d -states, with a *random* hopping between each of the sites of the lattice. We assume that the f and d states have a common chemical potential (μ) and interact by a Coulomb repulsion (U). In addition, both the d and f particles carry a spin label σ and the d -level can accommodate 2 electrons (or holes) of the opposite spin. The occupancy of the f -level is restricted to $n_f \leq 1$ because of the large Coulomb repulsion ($U_{ff} \sim \infty$) of the f -particles of opposite spins. To discuss the Yb-based VF compounds we use the hole-picture, in which $E < \mu$ and the total number of holes at the ill-placed sites is restricted to $n_h = n_d^h + n_f^h \leq 3$. In the electron-picture, one has $E > \mu$ and restricts the total number of electrons to $n_e = n_d^e + n_f^e \leq 3$. The magnetic field h couples to the f and d states but with different g -factors ($g = 4.5$ for the f -holes). This picture is described by a spin one-half Falicov-Kimball (FK) model [11],

$$\begin{aligned}
H = & \sum_{ij,\sigma} (t_{ij} - \mu \delta_{ij}) d_{i\sigma}^\dagger d_{j\sigma} + \sum_{i,\sigma} (E - \mu) f_{i\sigma}^\dagger f_{i\sigma} \\
& + U \sum_{i,\sigma\sigma'} d_{i\sigma}^\dagger d_{i\sigma'} f_{i\sigma'}^\dagger f_{i\sigma} + U_{ff} \sum_{i,\sigma} f_{i\uparrow}^\dagger f_{i\uparrow} f_{i\downarrow}^\dagger f_{i\downarrow} \\
& - \mu_B h \sum_{i,\sigma} \sigma (2d_{i\sigma}^\dagger d_{i\sigma} + g f_{i\sigma}^\dagger f_{i\sigma}) \quad , \quad (1)
\end{aligned}$$

where the notation of Ref. [12] is used and i and j denote the sublattice sites where the ill-placed Yb ions are located. The hopping matrix elements t_{ij} are chosen from a random distribution in such a fashion that as $N \rightarrow \infty$ the noninteracting density of states becomes Gaussian $\rho(\epsilon) = t^* \exp[-\epsilon^2/t^{*2}]/\sqrt{\pi}$ [13]. The only role of the regular lattice, with N_l sites, is to provide an infinite-range (random) connectivity between the sublattice sites.

In the limit $N \rightarrow \infty$ [14], and $N/N_l \ll 1$, our choice for t_{ij} maps this problem onto the infinite-dimensional (local) one, which allows the magnetic susceptibility to be evaluated exactly using the methods developed by Brandt and Mielsch [12]. The only differences we have is that we fix the total electron concentration (by adjusting μ) rather than fixing just the f -electron concentration. The Green's functions and susceptibilities are determined numerically by solving the self-consistent equations of Ref. [12]. The properties of the model depend on n_h , $E - \mu$, and U ; the value of the effective matrix element for random hopping (t^*) defines the energy scale. The uniform f-f spin-spin susceptibility satisfies $\chi_{SDW}^{ff}(T) = n_f^h(T)/2T$.

We present the susceptibility results of our numerical solutions for a variety of different cases in Figure 1. Each figure corresponds to a different value of n_h , with ten values of E/t^* ranging from 0 to -4.5 in steps of -0.5 . Fig. 1(a) is a typical high-density result. There are 2.5 holes per impurity site, implying $n_f^h \neq 0$ at all temperatures, leading to a Curie contribution to the susceptibility at small T . In this regime, the results are rather insensitive to U ($U = 10t^*$ here). Fig. 1(b) is the $n_h = 2.1$ case. We chose $U = t^*$ here, and the results depend sensitively on E , showing a downturn at moderate T , before the Curie-law divergence sets in for $T \rightarrow 0$. As n_h is decreased to 2 and beyond, it is no longer necessary for there to be any f holes remaining at $T = 0$, and χ^{ff} can vanish in that limit. In Fig. 1(c) we plot χ^{ff} for $n_h = 2$ and $U = 2t^*$, showing an asymmetric peak that increases in size and sharpens as T_V decreases, and which still has a weaker Curie upturn at the lowest temperatures, because $n_f^h \neq 0$ as $T \rightarrow 0$. Here, the results depend quite sensitively on E and U , with the peak lowering in magnitude and broadening as U increases, and the low-temperature upturn becoming more prominent. The case $n_h = 1.9$ is shown in Fig. 1(d) for $U = 10t^*$. Once again we have a sensitive dependence on the parameters, but the low-temperature upturn has disappeared. In some cases χ^{ff} has a double-hump structure. Finally the low-density regime is plotted in Fig. 1(e) ($n_h = 0.5$,

$U = 10t^*$). Here, as in the high-density limit, the results are insensitive to U .

The model also exhibits a metamagnetic transition, for large enough magnetic fields. This is shown in Figure 2 for one case: $n_h = 2$, $E = -t^*$, $U = 2t^*$, and eight temperatures from $0.05t^*$ up to $6.4t^*$. The numerical analysis shows that at $T = 0$, the Zeeman energy at the transition is of the order of $k_B T_V$. H_V decreases at higher temperatures but the transition becomes smoother. The metamagnetism disappears as T is increased beyond T_V , because the f -holes are already occupied in the zero-field limit.

The exact solution reproduces well the overall behavior of the experimental data. Figs.(1c)-(1d) capture most of the features shown by $\chi(T)$ in Refs. [1-3,6,7,9], such as an asymmetric peak at T_V that increases in magnitude and sharpens as $T_V \rightarrow 0$, while Fig.(2) explains $M(T)$ reported in [2,8], with a metamagnetic transition that smooths out and then disappears as T is increased. Various samples will have different numbers of Yb impurities and will require different values of the coupling constants. Our analysis shows that the lower the transition temperature, the more pronounced and steeper the anomaly. For large fields, unhybridized Yb ions crossover to a magnetic configuration at much lower temperatures, than in the absence of the field.

Although this is a complicated many-body system, in which the behavior depends strongly on the total number of particles at the impurity sites and the double occupancy of $4f$ -states is prohibited, the anomalous behavior can be understood in terms of simple thermodynamic considerations. For $E < \mu$ and $n_h < 2$, the nonmagnetic state of an Yb impurity is energetically more favorable than the magnetic state, so the ground state corresponds to the $4f^{14}$ configuration (no f -holes). However, at high T , the large entropy of the f -hole spins favors the magnetic state. Thus, the high-temperature response of an ensemble of Yb impurities approaches the limit $\chi_{local}(N, T) \simeq N\chi_0(T)$, where $\chi_0(T) \simeq (g\mu_B)^2/T$ is the local susceptibility of a single Yb ion with one unhybridized magnetic hole. The g -factor anisotropy of that hole gives rise to the field-induced torque which depends on temperature via $\chi_{local}(T)$. The anomalous part of the susceptibility and the torque grow rapidly as the temperature is reduced until, close to T_V , the entropy gain is insufficient to compensate the energy loss and the f holes are filled to form a nonmagnetic state. Thus, χ_{local} drops significantly, which is the origin of the sharp asymmetric peak in the $\Gamma(T)$ and $\chi(T)$ data. This anomalous peak conceals the broad maximum which is usually found in the susceptibility of VF compounds (from the electrons on the regular lattice). For $n_h \geq 2$, however, the f -hole cannot be completely filled at $T = 0$ and the residual f -spin leads to a low-temperature upturn of $\chi(T)$, which is also often seen in the data [1-3,6,7,9] (this theoretically predicted Curie tail will add to the Curie tail present in

all samples due to impurities). The associated Curie constant is very small for $n_h \simeq 2$ but increases rapidly as the density of holes increases. In YbInCu_4 , the proximity of the f -level to μ gives rise both to the FK-transition of unhybridized Yb ions and the VF behavior of hybridized Yb ions. Had $E - \mu$ been much larger than t^* , then the unhybridized f -levels would not change from $3+$ to $2+$ at low temperatures.

The transport properties are also explained by this scheme: the Kondo scattering for $T > T_V \gg T_K$ is at the spin-disorder limit, while for $T < T_V$ the free spins vanish and the Kondo scattering is absent. Hence, the resistivity jumps at T_V from its small low-temperature value to a high-temperature spin-disordered value [3]. The switching on and off of the Kondo scattering also leads to large anomalies in the elastic constants through the electron-phonon coupling at the regular lattice sites.

In summary, the response of YbInCu_4 and other Yb-based VF compounds is analyzed in terms of two independent magnetic excitations. The magnetic anomalies are attributed to an entropy-driven transition of disordered Yb and explained by the Falicov-Kimball model with random hopping. Although the disordered Yb ions undergo at T_V a large valence change, $\langle n_f \rangle$ does not change much since $N/N_l \ll 1$. Thus we account for the correlation between $\chi(T)$ and $\Gamma(T)$, explain the metamagnetic transition, and reconcile the large changes in magnetic, transport, and elastic properties with small changes in the f -count and the average atomic volume.

We acknowledge useful conversations with I. Aviani, Z. Fisk, M. Jarrell, B. Lüthi, M. Miljak, and J. Sarrao. J. K. F. acknowledges the Donors of The Petroleum Research Fund, administered by the American Chemical Society, for partial support of this research (ACS-PRF No. 29623-GB6) and the Office of Naval Research Young Investigator Program (N000149610828). This project has been funded in part by the National Research Council under the Collaboration in Basic Science and Engineering Program. The contents of this publication do not necessarily reflect the views or policies of the NRC, nor does mention of trade names, commercial products, or organizations imply endorsement by the NRC.

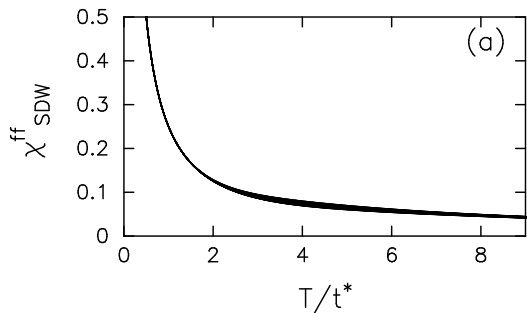
[†] Permanent address: Institute of Physics of the University of Zagreb, Croatia.

-
- [1] I. Felner and I. Novik., Phys. Rev. B **33**, 617 (1986); I. Felner, et al., Phys. Rev. B **35**, 6956 (1987).
 - [2] K. Yoshimura, et al., Phys. Rev. Lett. **60**, 851 (1988); T. Shimizu et al., J. Phys. Soc. Japan **57**, 405 (1988).
 - [3] B. Kindler, et al., Phys. Rev. B **50**, 704 (1994).
 - [4] K. Kojima, et al., J. Phys. Soc. Japan, **59**, 792 (1990).

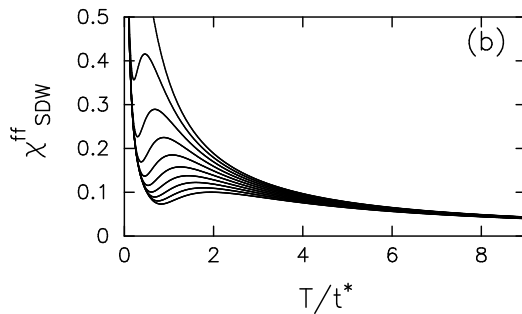
- [5] H. Nakamura, et al., J. Phys. Soc. Japan **59**, 28 (1990).
- [6] J.L. Sarrao et al., unpublished (1996)
- [7] J. M. Lawrence et al.; Phys. Rev. B, to appear (1996)
- [8] H.A. Katori, et al., Physica B, **201**, 159 (1994).
- [9] M. Miljak, et al., unpublished.
- [10] C. Rossel et al., Phys. Rev. B, **35**, 1914 (1987).
- [11] L. M. Falicov and J. C. Kimball, Phys. Rev. Lett. **22**, 997 (1969)
- [12] U. Brandt and C. Mielsch, Z. Phys. B **75**, 365 (1989); Z.Phys. B **79**, 295 (1990); U. Brandt, et al., Z.Phys. B **81**, 409 (1992).
- [13] We choose a Gaussian density of states rather than Wigner's semicircular density of states in order to include the effects of Lifshitz's tails. The theory is rather insensitive to the precise choice of $\rho(\epsilon)$. For details on this choice, see M. Moshe, H. Neuberger, and B. Shapiro, Phys. Rev. Lett. **73**, 1497 (1994); M. Kreyenin and B. Shapiro, Phys. Rev. Lett. **74**, 4122 (1995).
- [14] M. J. Rozenberg et al., Phys. Rev. B **49**, 10181 (1994).

FIG. 1. Magnetic susceptibility of the f -holes in the Falicov-Kimball model. The different curves correspond to $E/t^* = 0.0, -0.5, \dots, -4.5$ (in general E decreases from top to bottom in these figures). The different figures are: (a) $n^h = 2.5$ and $U = 10t^*$; (b) $n^h = 2.1$ and $U = t^*$; (c) $n^h = 2.0$ and $U = 2t^*$; (d) $n^h = 1.9$ and $U = 10t^*$; and (e) $n^h = 0.5$ and $U = 10t^*$.

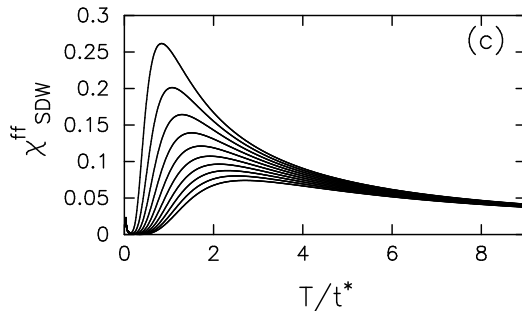
FIG. 2. Total magnetization of the Falicov-Kimball model as a function of magnetic field. The different curves correspond to different temperatures: $T/t^* = 0.05, 0.1, 0.2, \dots, 3.2, 6.4$ (the temperature increases from top to bottom in the large- h range). The parameters are $n^h = 2$, $E = -t^*$, and $U = 2t^*$.



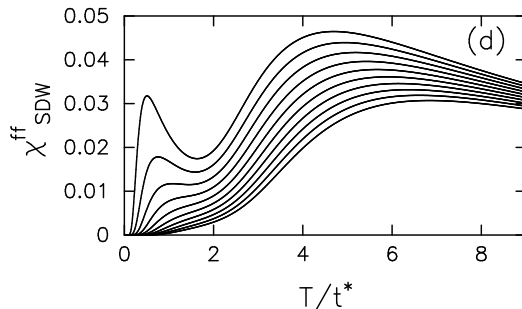
Freericks and Zlatic, Phys. Rev. Lett., Figure 1(a)



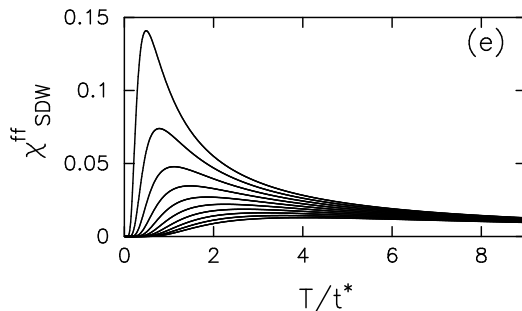
Freericks and Zlatic, Phys. Rev. Lett., Figure 1(b)



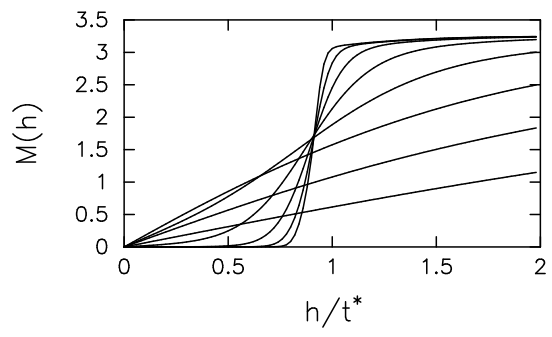
Freericks and Zlatic, Phys. Rev. Lett., Figure 1(c)



Freericks and Zlatic, Phys. Rev. Lett., Figure 1(d)



Freericks and Zlatic, Phys. Rev. Lett., Figure 1(e)



Freericks and Zlatic, Phys. Rev. Lett., Figure 2